Journal of Applied Polymer Science

Study of the Effect of Rutile/Anatase TiO_2 Nanoparticles Synthesized by Hydrothermal Route in Electrospun PVA/TiO_2 Nanocomposites

Rodrigo G. F. Costa,[1] Caue Ribeiro,[2] Luiz H. C. Mattoso[2]

[1]Departamento de Química, Universidade Federal de São Carlos, Via Washington Luiz km 235 São Carlos, SP 13560-970, Brazil

[2]Laboratório Nacional de Nanotecnologia Aplicada ao Agronegócio, Embrapa Instrumentação, Rua XV de Novembro, 1452 São Carlos, SP 13560-970, Brazil

Correspondence to: C. Ribeiro (E-mail: caue@cnpdia.embrapa.br)

ABSTRACT: Mixed rutile–anatase TiO_2 nanoparticles were synthesized by hydrothermal treatment under acidic conditions and incorporated into poly(vinyl alcohol) (PVA). These nanocomposites were electrospun to produce nanofibers of PVA/TiO_2, which were characterized by scanning electron microscopy, transmission electron microscopy, X-ray diffraction (XRD), UV–vis diffuse reflectance spectroscopy, thermogravimetric analysis, and differential scanning calorimetry. The photocatalytic degradation of Rhodamine B and degradation of the polymer by UV-C lamps were also investigated. The results showed that TiO_2 nanoparticles did not change the morphology and thermal behavior of the nanofiber polymer, but were effective in modifying the UV absorption of PVA without reducing its stability. © 2012 Wiley Periodicals, Inc. J. Appl. Polym. Sci. 000: 000–000, 2012

KEYWORDS: electrospinning; nanofibers; photocatalytic degradation; poly(vinyl alcohol); rutile–anatase nanoparticles

Received 3 February 2012; accepted 8 May 2012; published online
DOI: 10.1002/app.38031

INTRODUCTION

Electrospun poly(vinyl alcohol) (PVA) has recently been demonstrated to be a useful alternative to the bulk polymer, as its high surface area and mechanical properties are interesting for the applications of PVA such as textiles, biodegradable mats, and ultrafine separation filters.[1–3] By introducing inorganic nanofillers into this polymer, its properties may also be improved, and these nanoparticles can endow materials with remarkable properties such as electronic, antimicrobial, and catalytic activity.[4–10]

An especially interesting filler for nanocomposites is TiO_2 nanoparticles, as they offer special properties such as photocatalytic activity and, specially, the well-known effect of UV absorbance, which is used to protect polymers from solar light degradation.[6,11–13] Several groups have used poly(ethylene terephthalate),[14] poly(acrylonitrile) (PAN),[15] multiwalled carbon nanotube (MWCNT),[16] and fluoropolymer[17] as a polymer in nanocomposites. Prahsarn et al.[15] prepared PAN/TiO_2 anatase nanofibers web and investigated their photocatalytic activity. Peining et al.[16] fabricated MWCNT/TiO_2 nanocomposites with a morphology of rice grains. The authors observed that photodegradation of Alizarin Red Dye with the nanocomposites was better than TiO_2 rice grains and TiO_2 P-25.[16]

In a previous work from our research group, we studied the preparation of electrospun PVA/TiO_2 anatase nanocomposite fibers.[6] The immobilization of TiO_2 catalysts is still a challenge—to avoid the loss of material during the reaction processes. However, this strategy often implies in a significant reduction of the catalyst activity, as it reduces the total available area when compared with freestanding particles. Then, the electrospun structure may be an interesting way to immobilize TiO_2 nanoparticles in a high surface area substrate, which may be a good alternative to replace thin films of TiO_2. However, when we observed the action of this filler in the PVA fibers, we demonstrated that anatase nanoparticles (commercially supplied by Sigma-Aldrich) promoted the polymer degradation by UV light.[6] Actually, it is known[18,19] that anatase is photoactive, and generally, the rutile phase of TiO_2 is the most suitable to improve the resistance to UV. However, to the best of our knowledge, there are no published reports about PVA loaded with nanometric rutile TiO_2, as there are no regular commercial suppliers. On the other hand, it is notable that some studies report rutile TiO_2 nanoparticles as photoactive, which means that their introduction into the fibers may have the same deleterious effect as the anatase nanoparticles.[18,19]

In this work, we produced nanocomposite fibers loaded with synthesized TiO_2 nanoparticles in a mixture of both phases, that is, anatase and rutile, with the rutile phase predominating. The TiO_2 nanoparticles were produced by hydrothermal treatment of Ti–peroxocomplexes.[20] The results showed that the

rutile phase maintained its UV-protection capacity even as nanoparticles, indicating that this phase is promising for increasing the resistance of this electrospun material to UV radiation.

EXPERIMENTAL

Materials

PVA was purchased from J.T. Baker (87–89% hydrolyzed, average M_w = 11–31 kDa). Titanium metal powder and nitric acid were obtained from Sigma-Aldrich; hydrogen peroxide from Synth; and ammonia from Chemis. Deionized water (pH 6.5) was used as a solvent.

Synthesis of TiO_2 Nanoparticles by Hydrothermal Treatment Under Strongly Acidic Conditions (pH = 0) and Their Characterization

TiO_2 nanoparticles were synthesized as described by Ribeiro et al.[20] Titanium metal powder (Aldrich, St. Louis, MO, USA) (0.5 g) was added to 40 mL of concentrated ammonia and 120 mL of hydrogen peroxide (Synth, Brazil). This solution was placed in an ice-water bath for 12 h, resulting in a yellow solution of peroxytitanate $[(Ti(OH)_3O_2]^-$ ion, which was heated to boiling and then placed in an ice bath. The solution and the precipitate were frozen together and lyophilized. After drying the precipitate, an aliquot of ~ 0.2 g was stirred in a Teflon vessel with 100 mL of nitric acid (2 mol/L), resulting in a suspension at pH = 0, which was hydrothermalized for 2 h at 200°C and with a pressure of 14 bar in a controlled reactor. After the hydrothermal treatment, the TiO_2 nanoparticles were separated from the supernatant by centrifugation, washed, and dried by lyophilization. This material was characterized by X-ray diffraction (XRD), transmission electron microscopy (TEM), and dynamic light scattering (DLS), as described.

XRD patterns of TiO_2 nanoparticles were collected in a Shimadzu XRD600 with Ni-filtered Cu Kα radiation and scanned at 1°/min from 2θ = 5°–75°. The percentage of each phase in the anatase–rutile mixture was determined by the technique described in Refs. 18 and 21 using the following equations:

$$X_a = [1 + 1.26(I_r/I_a)]^{-1}, \quad (1)$$

$$X_r = 1 - X_a, \quad (2)$$

$$\%\text{Anatase} = X_a \times 100, \quad (3)$$

$$\%\text{Rutile} = X_r \times 100 \quad (4)$$

where X_a is the rate of anatase in the mixture, X_r is the rate of rutile in the mixture, I_a is the integrated intensity of the (101) reflection of anatase, and I_r is the integrated intensity of the (110) reflection of rutile. The size of titania crystallites was estimated by the Scherrer equation[18] from the broadening of the main anatase reflections and rutile reflections. These values are shown in Table I. The morphology of the TiO_2 nanoparticles was examined with a TEM (Philips CM 120). The sample was prepared by wetting copper–carbon grids with a drop of TiO_2 suspension and drying. The sizes of TiO_2 nanoparticles suspended in water (pH = 5.6, 25°C) were measured by DLS in a Zetasizer nanoparticle analyzer (Malvern Instruments).

Table I. Phase Composition of Synthesized Samples and Size of Titania Crystallites Estimated by the Scherrer Equation[18] from the Main Anatase Reflections and Rutile Reflections

	% Rutile	% Anatase	D_{rutile} (nm)	$D_{anatase}$ (nm)
Sample 1	59	41	31	34
Sample 2	59	41	33	38
Sample 3	51	49	37	36

Table II. Viscosity and Electrical Conductivity of PVA/TiO_2 Solutions

TiO_2 loading (wt TiO_2/wt PVA)	Viscosity (Pa s)	Conductivity (mS/cm)
0.0	0.19	1.41
2.5	0.29	1.54
5.0	0.35	1.59

Preparation of PVA/TiO_2 Nanocomposites by Electrospinning

Pure PVA solutions were prepared by dissolving the polymer (JT Baker, Phillipsburg, NJ, USA) in deionized water and stirred at 70°C for 2 h, yielding a transparent solution. The TiO_2 nanoparticles were incorporated into PVA by adding a known amount of TiO_2 powder to PVA aqueous solution and stirred for 2 h. As both materials are hydrophilic, it was not necessary to include any compatibilizing agent to assure good dispersion of TiO_2 nanoparticles in PVA. Thus, PVA (18 wt %) aqueous solutions were obtained with TiO_2 contents of 2.5 and 5.0 wt % (wt TiO_2/wt PVA). The electrical conductivity of PVA and PVA/TiO_2 solutions was measured with a Horiba ES 12 conductivity meter. The viscosities of all the solutions were measured with a rheometer (Anton Paar) at room temperature. These values are shown in Table II.

The method used in the PVA/TiO_2 aqueous solution electrospinning experiments was the same as in our previously published studies.[5,6] A voltage of 14 kV was applied to the solution, the working distance was set at 10 cm, the injection rate at 0.7 mL/h, and the collector speed at 200 rpm. The electrospinning was performed at room temperature and with 40–55% relative humidity. Webs of fibers were collected on aluminum foil and dried for 8 h at 60°C before characterization.

Characterization of the Nanocomposites

The morphology of all nanofibers was examined by scanning electron microscopy (SEM; Leo 440). The average fiber diameter and its standard deviation (SD) were determined in SEM images by direct measurement of at least 100 fibers using the software ImageJ.[22] TEM images of the PVA/TiO_2 (5 wt %) nanofibers were taken in a Philips CM 120 electron microscope, with an accelerating voltage of 120 kV. The samples were dispersed in a mixture of hexane and water (3 : 1 v/v), and a drop was deposited on a copper–carbon grid. The nanofiber crystal structures were examined by X-ray diffractometry (Shimadzu XRD 6000), with scans from 5° to 35° (2θ) at 0.05°/min, using Ni-filtered Cu Kα radiation.

The UV–vis diffuse reflectance spectra of nanofibers were recorded between 200 and 800 nm with a UV–vis-NIR

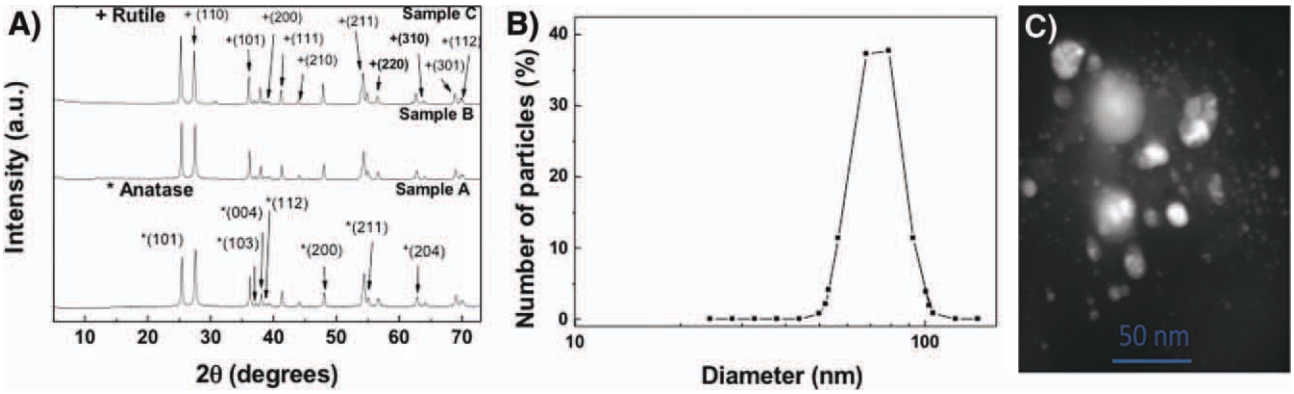

Figure 1. (A) X-ray diffraction patterns of TiO_2 nanoparticles prepared by 2 h of hydrothermal treatment under acidic conditions (pH = 0). (B) Size distribution of TiO_2 nanoparticles dispersed in water with 37 mg/L of TiO_2 at pH = 5.6. The sample was analyzed at 25°C. (C) TEM dark-field image of TiO_2 nanoparticles. [Color figure can be viewed in the online issue, which is available at wileyonlinelibrary.com.]

spectrophotometer (Varian Cary 5G). The values of the Kubelka–Munk function (k/S) were calculated by the following equation:

$$k/S = (1 - R\infty)^2/(2R\infty) \quad (5)$$

where S is the scattering coefficient, k is the absorption coefficient, and $R\infty$ is the reflectance from a layer of infinite thickness.[23]

A TGA Q500 (TA Instruments) was used for thermogravimetric analysis. The nanofibers were analyzed by heating from 25 to 600°C at 10°C/min under flowing nitrogen (40 mL/min). Differential scanning calorimetry (DSC) was performed with a TA Q100 calorimetry (TA Instruments) in nitrogen flowing at 50 mL/min. The DSC curves were recorded between 30 and 225°C at a heating rate of 10°C/min.

To evaluate the catalytic action associated with the TiO_2 nanoparticles in the fibers, photocatalytic degradation of Rhodamine B (RhB) was carried out in a box reactor with four UV-C lamps (100–280 nm). The sample was prepared by using about 0.0036 g of PVA/TiO_2 (5 wt %) nanofiber in 20 mL of a 2.5 mg/L dye solution in a beaker. In another beaker of the same solution, an equivalent mass of TiO_2 synthesized by the hydrothermal method was dispersed to produce a reference treatment. For comparison, an experiment was carried out in the absence of TiO_2. Spectra of the dye were measured by a UV–visible spectrophotometer (Shimadzu) with a variable wavelength (400–650 nm) using a quartz cell.

To evaluate possible degradation of PVA by the action of TiO_2 nanoparticles, a degradation experiment was carried out in the same box reactor with lamps UV-C as above. The temperature was about 25°C. The distance between the lamp and the samples was 12 cm. A 4-cm^2 nanofiber rectangular mat was cut as the sample, weighing 9.0–5.0 mg. The weight loss of PVA in the samples by photocatalytic degradation was monitored in duplicates and recorded against irradiation time.

RESULTS AND DISCUSSION

Figure 1(A) shows the XRD patterns of three samples of TiO_2 nanoparticles prepared by hydrothermal treatment for 2 h at pH 0, and Figure 1(B) shows the size distribution of a selected sample estimated by light scattering. It can be seen from the XRD patterns that in all the samples, only the anatase (*) and rutile (+) phases were detected, confirming the coexistence of two phases and showing that the desired phase, rutile, was present in the mixture.[18,24–26] However, when comparing the most intense diffraction reflection for each phase in the XRD patterns, anatase (101)[25] and rutile (110),[26] it is observed that the percentage of rutile in the anatase–rutile mixture varied with the sample, as shown in Table I. However, rutile was the majority component of the mixture in all cases (from 51 to 59%). These results agree with previous article published by Ribeiro et al.[20] We can also observe from Table I that the average diameters of titania crystallites estimated by the Scherrer equation[18] were in the range of 31–38 nm, which agrees in general with the TEM image of nanoparticles observed in Figure 1(C). The particle size measurements by DLS [Figure 1(B)] show sizes ranging from 50 to 100 nm. Considering this rather narrow range and the particles anisotropy, we may affirm that the nanoparticles are well dispersed in the water, with few agglomerates, which is highly desirable for their dispersion into the water-soluble PVA matrix.

A series of SEM images of the PVA nanofibers [PVA, PVA/TiO_2 (2.5 wt %) and PVA/TiO_2 (5 wt %)] are shown in Figure 2(A–C). It is clear that the nanofibers were randomly distributed in the mats and their morphology was uniform, without beads, showing that loading with TiO_2 did not interfere with the fiber production, at least in these amounts. TiO_2 nanoparticles will probably be well distributed in the nanofibers, in view of this uniform morphology. In fact, the TEM images of nanocomposite fibers indicate this good distribution, as seen in Figure 2(D), where the TiO_2 particles has the same morphology expected from the synthesized material.

The average diameter of each type of fiber was ranged from 100 to 119 nm [Figure 2(A–C)]. Taking the SDs into account, differences between the average diameters are negligible, indicating again that the presence of the nanoparticle did not affect the final fiber sizes. These results agree with our previous study,[6] in which it was shown that TiO_2 loading in PVA could interfere

Applied Polymer SCIENCE

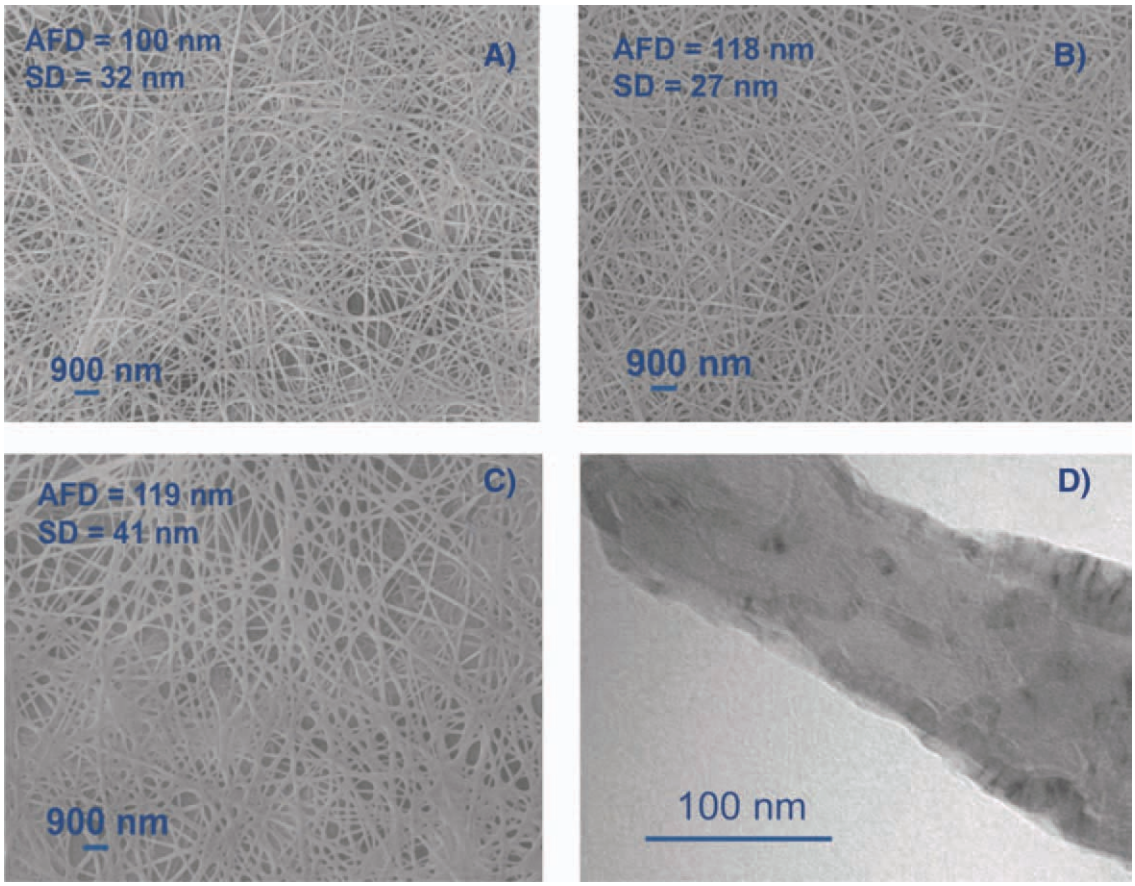

Figure 2. SEM images of nanofibers: (A) PVA, (B) PVA/TiO_2 (2.5 wt %), and (C) PVA/TiO_2 (5 wt %). (D) TEM bright-field image of PVA/TiO_2 (5 wt %) nanofiber. [Color figure can be viewed in the online issue, which is available at wileyonlinelibrary.com.]

with the spinning conditions only at very high concentrations, as it did not significantly change the solution conductivity (Table II). However, the viscosity of the PVA suspension was altered, which could interfere in the final fiber diameter at higher loadings; however, the slight variation within the range of loading in our study was unimportant.

The XRD patterns of the PVA nanofibers are shown in Figure 3. It can be seen that TiO_2 nanoparticles did not impede the crystallization path of the PVA phase, as expected. For all nanofibers, we can observe the PVA reflection at $2\theta = 19.5°$.[3,27] Besides the diffraction reflection for PVA, the major reflections of anatase and rutile are observed at $2\theta = 25.4°$ and $28°$.[25,26] However, we could not see other reflections from the anatase[25] and rutile phases,[26] owing to low TiO_2 contents. The UV–vis diffuse reflectance spectra (Figure 4a and b) indicate the presence of TiO_2 nanoparticles in the nanofibers. The absorption of the PVA/TiO_2 nanocomposites in the UV region was also higher than that of the PVA nanofiber, which confirms the expected UV absorption effect desirable for the improvement of resistance to UV irradiation.

To characterize the thermal behavior of PVA nanofibers, TG, DTG, and DSC analyses were carried out. The TG curves showed that the TiO_2 loading did not change the thermal degradation mechanism for this polymer. The presence of nanoparticles only increased the final residue, as expected. These results were corroborated by DTG curves [Figure 5(A)], which showed two weight loss steps during degradation: the main weight loss around 240–350°C is associated with dehydration of the polymer side chain, whereas the loss from 370–485°C reflects the loss of residual acetate groups on the side chains of the polymer.[28] DSC analysis corroborated with these results, as it showed the same melting temperature, 190°C, for all the nanocomposites [Figure 5(B)].[28,29] The endothermic peaks around 100–115°C relate to the evaporation of free water and should not be correlated to any specific behavior of the nanocomposite itself, as PVA is highly hydrophilic.

To evaluate the surface accessibility of TiO_2 nanoparticles dispersed in the fibers, a catalytic experiment was performed, using RhB as a probe of the TiO_2 activity.[6] As only the nanoparticles attached to the surface are expected to have some activity in the degradation of the dye, the catalytic experiment is a way of indirectly analyzing the distribution of TiO_2 in the fibers. Figure 6(A) shows the photocatalytic degradation of RhB under eight sets of conditions. It can be seen that the degradation of dye after 30 min with PVA/TiO_2 (5 wt %) was slightly greater than that of the self-sensitization of RhB; however, after 7 h of UV irradiation, the dye was more degraded by self-sensitization than with the fiber. This effect is probably due to the fact that

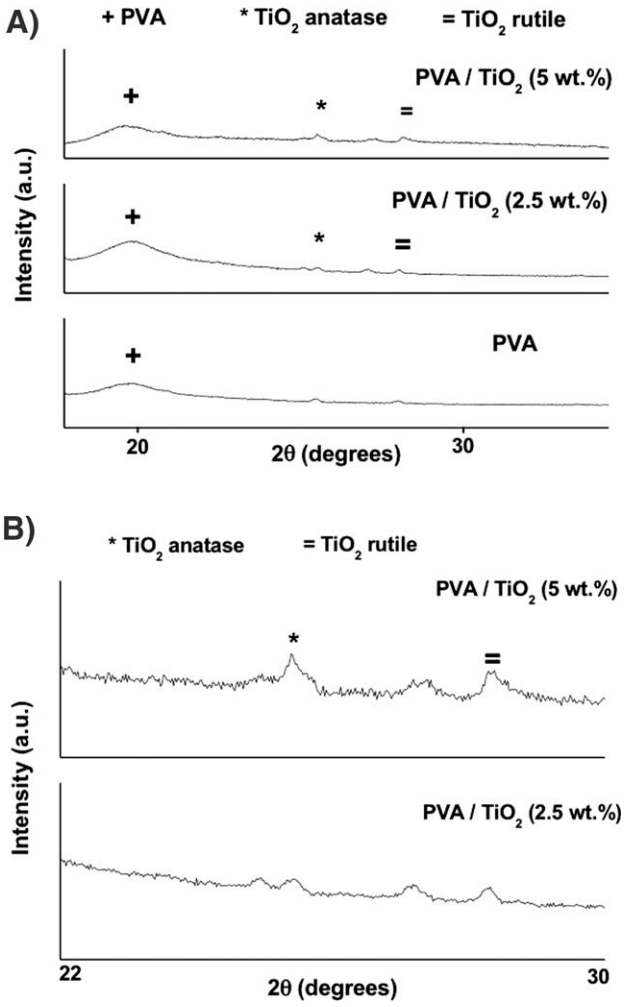

Figure 3. (A) X-ray diffraction patterns of electrospun nanofibers: PVA/TiO_2 (5 wt %), PVA/TiO_2 (2.5 wt %), and PVA. (B) Detail of the region $2\theta = 22°–30°$.

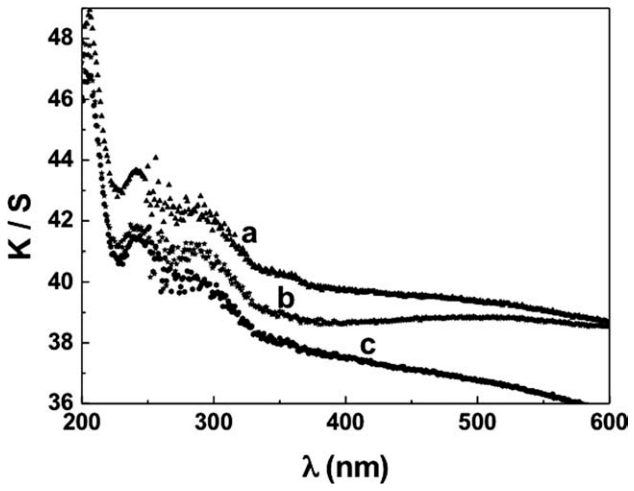

Figure 4. UV–vis diffuse reflectance spectra for (a) PVA/TiO_2 (5.0 wt %), (b) PVA/TiO_2 (2.5 wt %), and (c) PVA.

the nanocomposite absorbs some radiation or the TiO_2 nanoparticles degrade the PVA, in competition with the degradation of RhB.[6] In the comparison of equivalent amounts of TiO_2 in the nanofiber and as a dispersed powder in suspension, after 30 min and 7 h, we observe that the degradation of RhB by the dispersed powder condition was greater than the degradation with nanofiber. It is important to mention that despite the synthesized TiO_2 nanoparticles presented a worse performance for the dye degradation when compared with a commercial anatase nanopowder, they had a significant photodegradation activity, as shown in the figure.

This behavior showed that the majority of TiO_2 particles were inside the fibers and confirmed the UV absorption effect associated with these low TiO_2 loadings. However, as the synthesized particles showed some low photocatalytic activity, it was very important to assess the UV degradation of PVA by the filler. Figure 6(B) shows that the mass loss was negligible, contrary to the result in our previous study,[6] in which a TiO_2 anatase loading promoted a severe mass loss, especially in the first

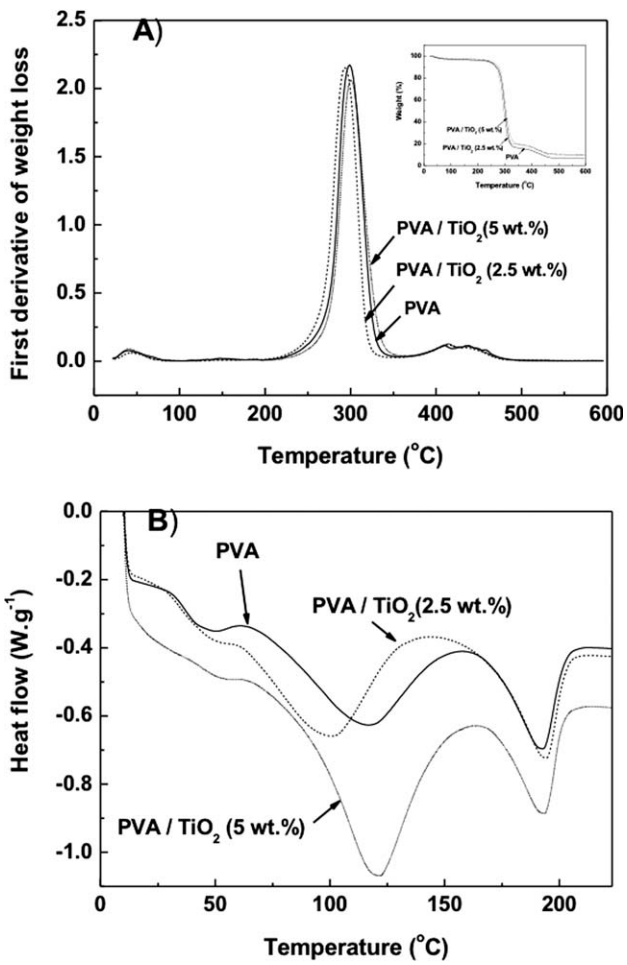

Figure 5. (A) DTG curves of electrospun nanofibers with inset thermogravimetric curves: PVA, PVA/TiO_2 (2.5 wt %), and PVA/TiO_2 (5 wt %). (B) DSC thermograms of electrospun nanofibers: PVA, PVA/TiO_2 (2.5 wt %), and PVA/TiO_2 (5 wt %).

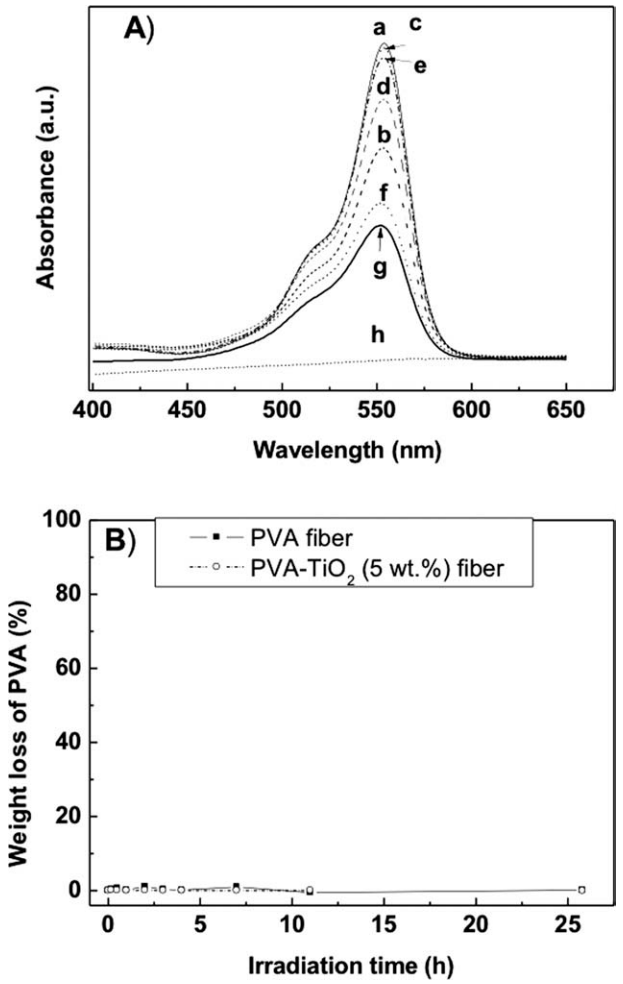

Figure 6. (A) Rhodamine B photocatalytic degradation by UV-C under various conditions: (a) RhB (30 min), (b) RhB (7h), (c) RhB with PVA/TiO_2 (5 wt.%) fiber (30 min), (d) RhB with PVA/TiO_2 (5 wt.%) fiber (7 h), (e) RhB with TiO_2 synthesized by hydrothermal method (30 min), (f) RhB with TiO_2 synthesized by hydrothermal method (7h), (g) RhB with bare TiO_2 (anatase) (30 min), (h) RhB with bare TiO_2 (anatase) (7h). (B) Weight loss of PVA: PVA fiber and PVA/TiO_2 (5 wt.%) fiber under UV-C light against irradiation time in air.

degradation times. Arantes et al.[30,31] also observed a similar degradation effect when loading styrene–butadiene rubber with synthetic TiO_2 anatase. The current result is very important, as it shows that the rutile TiO_2 synthesized, despite being in a mixture with some anatase, was effective in modifying the UV absorption behavior of PVA, without negatively affecting the PVA stability.

SUMMARY

We successfully prepared PVA/TiO_2 nanocomposite fibers by electrospinning, with average diameters in the range of 100–119 nm. The morphology of electrospun PVA/TiO_2 nanocomposite was uniform and without beads. It was observed that the polymer loaded with a low percentage of TiO_2 rutile–anatase nanoparticles did not alter the thermal behavior or impede the crystallization of PVA. The surface accessibility of dispersed TiO_2 nanoparticles in the fibers was probed by degradation of RhB. The nanoparticles were observed to be active in absorbing UV radiation, which is desirable to improve the resistance of the polymer to UV irradiation.

ACKNOWLEDGMENTS

The authors acknowledge the financial support of CAPES, CNPq, FAPESP, and FINEP.

REFERENCES

1. Chowdhury, M.; Stylios, G. J. *Mater. Sci.* **2011,** *46*, 3378.
2. Supaphol, P.; Chuangchote, S. J. *Appl. Polym. Sci.* **2008,** *108*, 969.
3. Shao, C.; Kim, H. Y.; Gong, J.; Ding, D.; Lee, D. R.; Park, S. J. *Mater. Lett.* **2003,** *57*, 1579.
4. Feng, Q.; Dang, Z.; Li, N.; Cao, X. *Mater. Sci. Eng. B* **2003,** *99*, 325.
5. Costa, R. G. F.; Ribeiro, C.; Mattoso, L. H. C. Sci. *Adv. Mater.* **2010,** *2*, 157.
6. Costa, R. G. F.; Ribeiro, C.; Mattoso, L. H. C. J. Nanosci. Nanotechnol. **2010,** *10*, 5144.
7. He, C. H.; Gong, J. *Polym. Degrad. Stab.* **2003,** *81*, 117.
8. Wu, H.; Fan, J.; Qin, X.; Zhang, G. *Mater. Lett.* **2008,** *62*, 828.
9. Lee, K.; Lee S. J. *Appl. Polym. Sci.* **2012,** *124*, 4038.
10. Linh, N. T. B.; Lee, K. H.; Lee, B. T. *J. Mater. Sci.* **2011,** *46*, 5615.
11. Whang, Z.; Li, G.; Peng, H.; Zhang, Z.; Wang, X. J. *Mater. Sci.* **2005,** *40*, 6433.
12. Zhao, X.; Lv, L.; Pan, B.; Zhang, W.; Zhang, S.; Zhang, Q. *Chem. Eng. J.* **2011,** *170*, 381.
13. Ning, W.; Jiaxi, W.; Qufu, W.; Ybing, C.; Bing, L. *e-Polymers* **2009,** *152*.
14. Xiangfu, M.; Xiaoying, F.; Zhongfeng, L.; Ying, Z. *Curr. Nanosci.* **2012,** *8*, 3.
15. Prahsarn, C.; Klinsukhon, W.; Roungpaisan, N. *Mater. Lett.* **2011,** *65*, 2498.
16. Peining, Z.; Nair, A. S.; Shengyuan, Y.; Ramakrishna, S. *Mater. Res. Bull.* **2011,** *46*, 588.
17. He, T.; Zhou, Z.; Xu, W.; Ren, F.; Ma, H.; Wang, J. *Polymer* **2009,** *50*, 3031.
18. Koleńko, Y. V.; Churagulov, B. R.; Kunst, M.; Mazerolles, L.; Justin, C. C. *Appl. Catal. B: Environ.* **2004,** *54*, 51.
19. Mourao, H. A. J. L.; Mendonça, V. R.; Malagutti, A. R.; Ribeiro, C. *Quim. Nova.* **2009,** *32*, 2190.
20. Ribeiro, C.; Barrado, C. M.; Camargo, E. R.; Longo, E.; Leite, E. R. *Chem. Eur. J.* **2009,** *15*, 2217.
21. Spurr, R. A.; Myers, H. *Anal. Chem.* **1957,** *29*, 760.
22. Software ImageJ. Available at: http://rsbweb.nih.gov/ij/index.html. Accessed on September 20, **2011.**
23. Gonçalves, I. G.; Petter, C. O. *Rev. Esc. Minas.* **2007,** *60*, 491.

24. Inada, M.; Mizue, K.; Enomoto, N.; Hojo, J. *Sci. Adv. Mater.* **2010,** *2*, 102.
25. Joint Committee on Powder Diffraction Standards database, card number 21-1272 (anatase TiO_2).
26. Joint Committee on Powder Diffraction Standards database, card number 21-1276 (rutile TiO_2).
27. Brandrup, J.; Immergut, E. H.; Grulke, E. A.; Akihiro, A.; Daniel, R. B. Polymer Handbook, 4th ed.; Wiley: New York, **1999.**
28. Pheng, Z.; Kong, L. X. *Polym. Degrad. Stab.* **2007,** *92*, 2007.
29. Guerrini, L. M.; Oliveira, M. P.; Branciforti, M. C.; Custódio, T. A.; Bretas, R. E. *S. J. Appl. Polym. Sci.* **2009,** *112*, 1680.
30. Arantes, T. M.; Leite, E. R.; Longo, E.; Camargo, E. R. *J. Appl. Polym. Sci.* **2009,** *113*, 1898.
31. Arantes, T. M.; Leão, K. V.; Tavares, M. I. B.; Ferreira, A. G.; Longo, E.; Camargo, E. R. *Polym. Test.* **2009,** *28*, 490.